Optical and Quantum Electronics (2019) 51:331
https://doi.org/10.1007/s11082-019-2018-2

Effect of the electric field induced birefringence on the slab waveguide evanescent-wave sensor sensitivity

A. Cherouana[1,2] · A. Bencheikh[3] · I. Bouchama[1]

Received: 5 March 2019 / Accepted: 27 August 2019

Abstract
We have investigated the potential of using the E-field induced birefringence for improving the sensitivity of uniaxial anisotropic slab waveguide sensor based on evanescent wave interactions. $LiNbO_3$ waveguide core was used as an example. We have calculated the sensor sensitivity formulas for the two kinds of modes propagating simultaneously in the waveguide sensor. In our study, we have distinguished between two different cases. The first case when the electric field is applied along the optic axis (+c) of the $LiNbO_3$ wave guiding film (positive electric field); the second case when the electric field is applied opposite to the optic axis (−c) of such uniaxial crystal (negative electric field). The obtained results showed that, for positive electric field, increasing the electric field induces an increasing of the total anisotropy which causes decreasing on sensor sensitivity. However, for negative electric field, the increase of absolute values of negative electric field induces a decrease of the total anisotropy, the latter increases the sensor sensitivity. On the other hand, the study of the physical parameters on the sensor sensitivity showed that, to maximize the sensor sensitivity, it is advisable to use isotropic substrate that has a refractive index as closer as possible to the measurand index.

Keywords Evanescent wave · Induced birefringence · Planar waveguide sensor · Sensor sensitivity · Uniaxial anisotropy

✉ A. Bencheikh
Bencheikhabdelhalim1976@Gmail.com

A. Cherouana
acherouana@cdta.dz

[1] Department of Electronics, University of Mohamed BOUDIAF, M'sila, Algeria

[2] Research Unity in Optics and Photonics, Center of Development of Advanced Technologies, University of Sétif 1, Algiers, Algeria

[3] Department of Electromechanics, University of BBA, Bordj Bou Arreridj, Algeria

Published online: 26 September 2019

1 Introduction

Planar waveguide optical sensors offer various advantages such as rapid response, immunity to electromagnetic interference, compactness, high sensitivity, low cost and they are easy to interface with optical data communication systems. When light propagates in the waveguide, a fraction of the radiation extends a short distance from the guiding region into the medium of lower refractive index which surrounds it. This evanescent wave which decays exponentially with distance from the waveguide interface defines a sensing volume within which the evanescent energy may interact with chemical and biological molecules (Dutta et al. 2016); based on this principle, slab waveguide optical chemical sensors (Ranacher et al. 2016; Huang et al. 2014) and biosensors (Mukundan et al. 2009; Horvath et al. 2003) were studied. Sensitivity enhancement of optical sensors based on evanescent wave interactions has attracted significant research interest. Therefore, a normalized analysis for the design of evanescent wave sensors was carried out, and the condition for the maximum achievable sensitivity was derived for both linear TE and TM waveguide sensors (Parriaux and Dierauer 1994). Then, it has been demonstrated that the sensitivity of a three-layer slab waveguide sensor can be larger than unity in the case of TM polarization and strong guidance (Veldhuis et al. 2000). In addition to that, a new highly sensitive evanescent field sensor using silicon-on-insulator (SOI) photonic wire waveguides was demonstrated (Densmore et al. 2006). Furthermore, sensitivity analysis of the nonlinear asymmetric metal-clad planar waveguide-based sensor was reported (Kumar and Singh 2011), it has been shown that the introduction of the nonlinear material in the cover media not only improves the sensitivity but also provides additional parameters to increase the sensitivity. Recently, binary and ternary photonic crystal with left-handed material (LHM) layers and multi-layer slab waveguides comprising LHMs with different configurations, have been investigated as optical sensors. It has been found that the sensitivity of the proposed structures can be significantly improved by the optimization of physical and geometrical parameters of the LHM layers (Taya and Shaheen 2018; Taya 2014, 2015a, b, 2018; Taya et al. 2009; Alkanoo and Taya 2018). On the other hand, many integrated optics and sensor applications use crystalline film guides with anisotropic optical properties, the dielectric medium is anisotropic either naturally so or due to applied external fields. The simplest types of anisotropic materials are the uniaxial anisotropic crystals known as birefringent materials. The birefringence takes place when the electromagnetic waves propagate in a medium which exhibits two distinct refractive indexes, in a same wave vector direction. Lithium Niobate (LN) is a high refractive index birefringent crystal with tunable optical properties. It is widely used for integrated optics and sensor applications due to its excellent ferroelectrical, piezoelectrical, and thermoelectrical properties; its transparency over a wide wavelength range (350–5200 nm), its nonlinear optical polarizability, and its Pockels effect (Kovalevich et al. 2017), especially after the fabrication of $LiNbO_3$thin film crystals having an optical quality and electrooptical coefficients comparable to bulk crystals (Levy et al. 1998). Thing that allowed the production of a $LiNbO_3$ slab waveguide structure, where the coupling of TE and TM modes into a such waveguide was observed (Rabieia and Gunter 2004).

In this work we investigate mainly, the potential of using the E-field induced birefringence for improving the sensitivity of uniaxial anisotropic slab waveguide sensor. The core of the waveguide, media above and below the guiding film, are constituted of uniaxial anisotropic crystals. Firstly, the characteristic equations of TE and TM modes are calculated, and the two expressions of the sensitivity are derived in the case where

the material above the guide film is isotropic. Finally, the influence of E-field induced birefringence of the wave guiding film constituted by $LiNbO_3$, on the sensor sensitivity, is investigated for the two fundamentals modes. Our study is concerned two cases. The first case when the electric field is applied along the optic axis (+c) of the $LiNbO_3$ wave guiding film (positive electric field); the second case when the electric field is applied opposite to the optic axis (−c) of such uniaxial crystal (negative electric field). The influence of the physical parameters of the slab waveguide on the sensor sensitivity is also studied.

2 Theoretical modeling

2.1 Characteristic equations calculation

Planar optical waveguides are the basic element in building integrated optical sensors. In following we consider a slab waveguide constituted by three layers uniaxial crystals as presented in Fig. 1. We consider that the materials of the three layers are lossless and non-magnetic. The core permittivity tensor is $\overline{\overline{\varepsilon}}_f$ with its optic axis in the direction of propagation z. The permittivity tensors of the media above and below the film guide are $\overline{\overline{\varepsilon}}_p$ and $\overline{\overline{\varepsilon}}_s$ respectively, where

$$\overline{\overline{\varepsilon}}_i = \begin{bmatrix} \varepsilon_i & 0 & 0 \\ 0 & \varepsilon_i & 0 \\ 0 & 0 & \varepsilon_{iz} \end{bmatrix} = \varepsilon_0 \begin{bmatrix} n_i^2 & 0 & 0 \\ 0 & n_i^2 & 0 \\ 0 & 0 & n_{iz}^2 \end{bmatrix} \tag{1}$$

Notice that ε_0 is the dielectric constant of vacuum, i = p, f, s (cover, film, substrate),$n_i = n_{ix} = n_{iy}$, n_{iz} are, respectively, the ordinary and the extraordinary refractive indices of each layer.

Two waves are propagated separately in the core of such slab waveguide, the ordinary wave, considered as a TE wave and the extraordinary wave considered as a TM wave (Jalaleddine 1982).

Using Maxwell's equations, constitutive relations and boundary conditions, the characteristic equations of TE and TM waves are obtained (detailed calculation can be found in Jalaleddine 1982) as follows

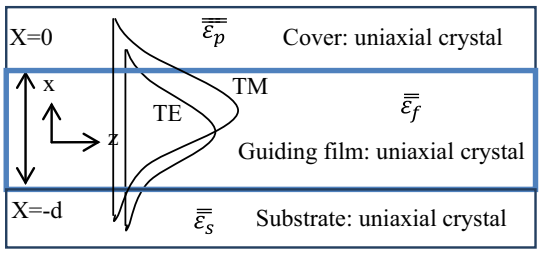

Fig. 1 Uniaxial anisotropic slab waveguide based sensor

For TE modes it's given by

$$k_0 d\sqrt{n_f^2 - N^2} = arctan\left(\sqrt{\frac{N^2 - n_s^2}{n_f^2 - N^2}}\right) + arctan\left(\sqrt{\frac{N^2 - n_p^2}{n_f^2 - N^2}}\right) + m\pi \tag{2}$$

For TM modes it is

$$k_0 d\frac{n_{fz}}{n_f}\sqrt{n_f^2 - N^2} = arctan\frac{n_{fz}n_f}{n_{pz}n_p}\sqrt{\frac{N^2 - n_p^2}{n_f^2 - N^2}} + arctan\frac{n_{fz}n_f}{n_{sz}n_s}\sqrt{\frac{N^2 - n_s^2}{n_f^2 - N^2}} + m\pi \tag{3}$$

where N is the effective refractive index, m is the mode order, d is the core thickness and k_0 is the free-space wavenumber.

2.2 Sensitivity of uniaxial anisotropic planar waveguide sensor

The sensitivity is defined as the rate of change of the modal effective refractive index relative to the cover refractive index, $S = \left(\frac{\partial n_p}{\partial N}\right)^{-1}$ (we consider that the cover layer is isotropic, that's means: $n_p = n_{pz}$). By differentiating the characteristics Eqs. (2) and (3) with the last consideration, and after long algebra we found the sensor sensitivity for TE and TM modes, by taking into account the normalization as in (Veldhuis et al. 2000).

For TE modes, the sensitivity is given by

$$S_{TE} = \sqrt{\frac{1 - a_p}{1 - X}}\frac{X}{a_p}\frac{1}{\sqrt{a_p - X}}\frac{1}{\left[T + \frac{1}{\sqrt{a_s - X}} + \frac{1}{\sqrt{a_p - X}}\right]} \tag{4}$$

In the same manner, the sensitivity for TM modes is given by

$$S_{TM} = \frac{\frac{X(1-2X+a_p)\sqrt{1-a_p}}{\sqrt{1-X}\sqrt{a_p-X}[a_p(1-X(1-Xa_{pz}))-Xa_{pz}]}}{\left[T'K + \frac{a_p(1-a_p)}{\sqrt{(a_p-X)}[a_p(1-X(1-Xa_{pz}))-Xa_{pz}]} + K\sqrt{\frac{1-a_{sz}}{1-a_s}}\frac{a_s(1-a_s)}{\sqrt{(a_s-X)}[a_s(1-X(1-Xa_{sz}))-Xa_{sz}]}\right]} \tag{5}$$

where

$$T = \frac{arctan\sqrt{\frac{a_s - X}{X}} + arctan\sqrt{\frac{a_p - X}{X}} + m\pi}{\sqrt{X}} \tag{6}$$

$$T' = \frac{arctan\frac{1}{\sqrt{1-a_p}\sqrt{1-a_{pz}}}\sqrt{\frac{a_p - X}{X}} + arctan\frac{1}{\sqrt{1-a_s}\sqrt{1-a_{sz}}}\sqrt{\frac{a_s - X}{X}} + m\pi}{\sqrt{X}} \tag{7}$$

$$a_s = 1 - \frac{n_s^2}{n_f^2} \tag{8}$$

$$a_p = 1 - \frac{n_p^2}{n_f^2} \tag{9}$$

$$X = 1 - \frac{N^2}{n_f^2} \tag{10}$$

$$a_{sz} = 1 - \frac{n_{sz}^2}{n_{fz}^2} \tag{11}$$

$$a_{pz} = 1 - \frac{n_p^2}{n_{fz}^2} \tag{12}$$

$$K = \frac{n_{fz}}{n_f} \tag{13}$$

2.3 Electric-field-induced birefringence of uniaxial crystals

It is well-known that electric fields can alter the refractive index of certain materials via the Pockels effect. When an electric field E is applied along (or opposite) the optic axis (c) of Trigonal 3 m uniaxial Crystals (as $LiNbO_3$), the crystal remains uniaxial with the same principal axes, but its refractive indices are modified. We distinguish two cases according to the direction of the applied electric field. If the electric field is applied along the optic axis (+c), then refractive indices are modified as (Saleh and Teich 1991)

$$n_0(E) \approx n_0 - \frac{1}{2} n_0^3 r_{13} E \tag{14}$$

$$n_e(E) \approx n_e - \frac{1}{2} n_e^3 r_{33} E \tag{15}$$

However, if the electric field is applied opposite to the optic axis (-c) of such uniaxial crystal, its refractive indices are modified as

$$n_0(E) \approx n_0 + \frac{1}{2} n_0^3 r_{13} E \tag{16}$$

$$n_e(E) \approx n_e + \frac{1}{2} n_e^3 r_{33} E \tag{17}$$

where n_0 and n_e are the ordinary and extraordinary refractive indices of the uniaxial crystal without the application of electric field E, $n_0(E)$ and $n_e(E)$ are respectively the modified ordinary and extraordinary refractive indices of the uniaxial crystal with the application of electric field, r_{13} and r_{33} are the linear electro-optic coefficients of the medium.

For this trigonal 3 m uniaxial Crystal ($LiNbO_3$), the total birefringence as defined by Timtere et al. (2011) is given as

$$\Delta n(E) = \left| n_{high}(E) - n_{low}(E) \right| \tag{18}$$

For a positive applied electric field (according +c), the corresponding total birefringence is

$$\Delta n(E) = \left| n_0 - n_e + \frac{1}{2} E\left(n_e^3 r_{33} - n_0^3 r_{13} \right) \right| \tag{19}$$

We know that all Pockels media have r_{33} greater than $r_{13}(r_{33} > r_{13})$. This means that total birefringence $\Delta n(E)$ is a linear increasing function of E.

For negative applied electric field (according −c), the corresponding total birefringence is

$$\Delta n(E) = \left| n_0 - n_e + \frac{1}{2} E\left(n_0^3 r_{13} - \frac{1}{2} n_e^3 r_{33} \right) \right| \tag{20}$$

While $r_{33} > r_{13}$ This means that total birefringence $\Delta n(E)$ is a linear decreasing function of E.

Noting that, typical optical properties of $LiNbO_3$ are given in Table 1.

3 Results and discussion

3.1 Influence of physical parameters on the sensor sensitivity

Figure 2 shows the sensitivity variation of the fundamental modes, for a slab waveguide sensor as a function of frequency for different values of the cover index n_p; the core of the waveguide sensor is $LiNbO_3$($n_{fx} = 2.2880$, $n_{fz} = 2.2030$), the substrate is the glass $n_s = 1.48749$; for the first look on the graph it is clear that sensitivities of TM_0 mode (markers with linked lines curves) are more important than those of TE_0 mode (markers without linked lines curves), further, maximum sensitivities of TM_0 mode are situated in the visible domain of frequency; whereas those of TE_0 mode are situated in the near infrared domain. In addition to that, for TE_0 and TM_0 modes, the sensitivity of the sensor increases by making the cover index n_p closer to that of the substrate n_s, consequently a shift of the curves towards the near-infrared frequencies is noticed.

Figure 3 shows a comparison between sensitivities of two different sensors constituted with the same $LiNbO_3$ core; and two different substrates, the substrate of the

Table 1 Optical properties of $LiNbO_3$ at 632.8 nm

n_0	n_e	r_{13} (10^{-12} mV^{-1})	r_{33} (10^{-12} mV^{-1})
2.2880	2.2030	10	32.2

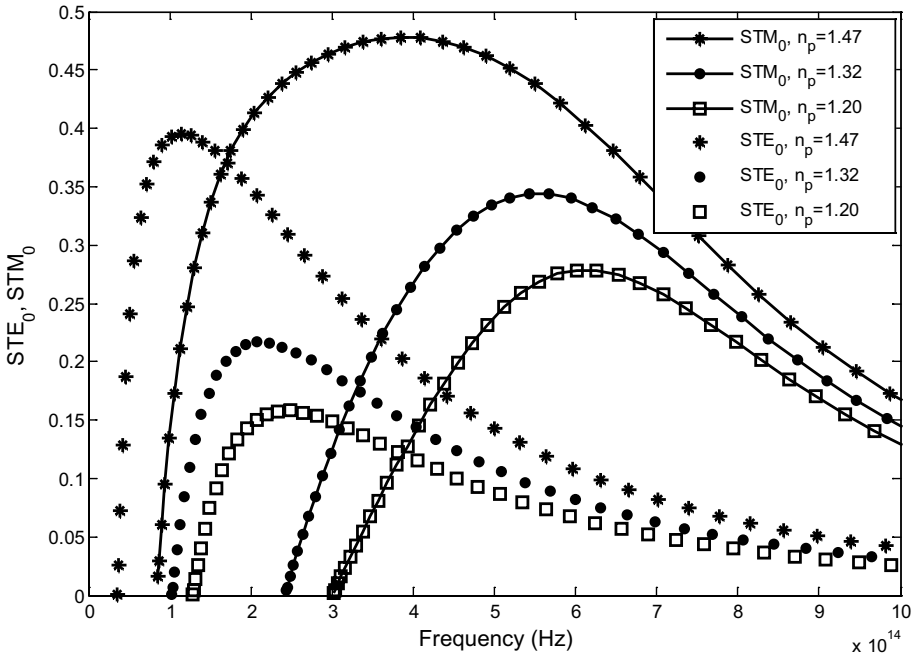

Fig. 2 Sensitivity as a function of the frequency for TE_0 and TM_0 modes for different refractive index of cover materials n_p, markers with linked lines curves for TM_0 mode and markers without linked lines curves for TE_0 mode ($n_s = 1.48749$, d = 100 nm, $LiNbO_3$ as guiding film)

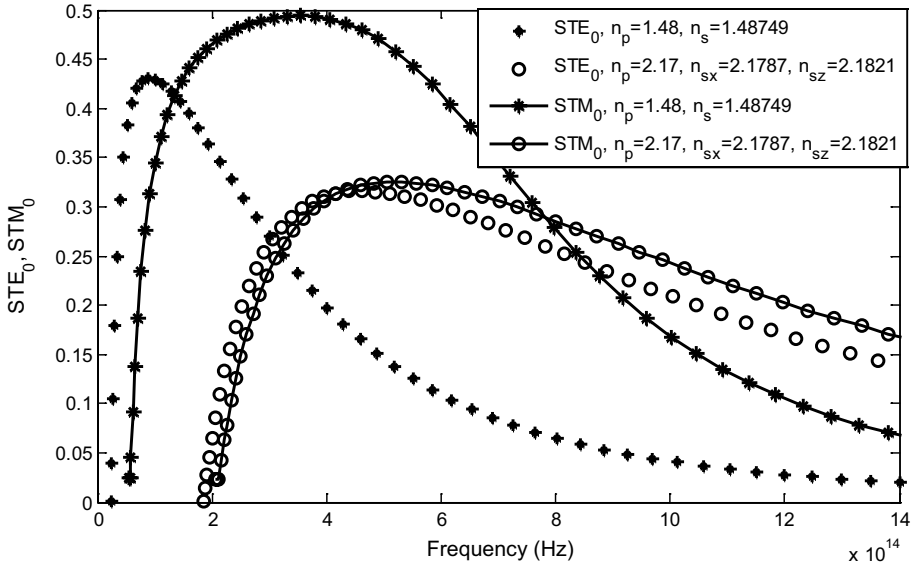

Fig. 3 Sensitivity as a function of the frequency for TE_0 and TM_0 modes for two different substrate materials (curves in stars for isotropic glass $n_s = 1.48749$ and curves in circles for uniaxial $LiTaO_3$, $n_{sx} = 2.1787$, $n_{sz} = 2.1821$), d = 100 nm, $LiNbO_3$ as guiding film

first sensor is isotropic (glass) whereas, that of the other sensor is uniaxial anisotropic ($LiTaO_3$). It is found that, for the two fundamental modes (TE_0 and TM_0), the sensitivity of the sensor constituted by isotropic substrate (curves in stars) is greater than that of the sensor constituted by uniaxial substrate (curves in circles), In addition to that, the curves of the sensitivity shift towards the UV frequencies if the substrate is uniaxial anisotropic; it is worth to note that the shift of the TE_0 mode curve (markers without linked lines curves) is more important than the shift of the TM_0 mode curve (markers with linked lines curves).

3.2 Influence of E-field induced birefringence on the sensor sensitivity

As we have seen previously, the natural anisotropy of $LiNbO_3$birefringent material, changes with the application of an external electric field. Indeed, if the applied electric field is positive (according +c), the total birefringence is an increasing function of E (Eq. 19). While, if the applied electric field is negative (according −c), the total birefringence is a decreasing function of E (Eq. 20). To see the influence of birefringence variation on the sensor sensitivity for both positive and negative applied electric field, theoretically, we take arbitrary three values of $\Delta n(E)$ for each case; the values of $n_0(E)$ and $n_e(E)$ are deduced from their corresponding equations. We have traced the sensitivities of the sensors as a function of frequency for the three values of $\Delta n(E)$.

Figures 4 and 5 present respectively, fundamental modes sensitivities as a function of the frequency for different values of total birefringence induced by different values of positive and negative electric field. The curves of sensitivities, for TE_0 or TM_0, show

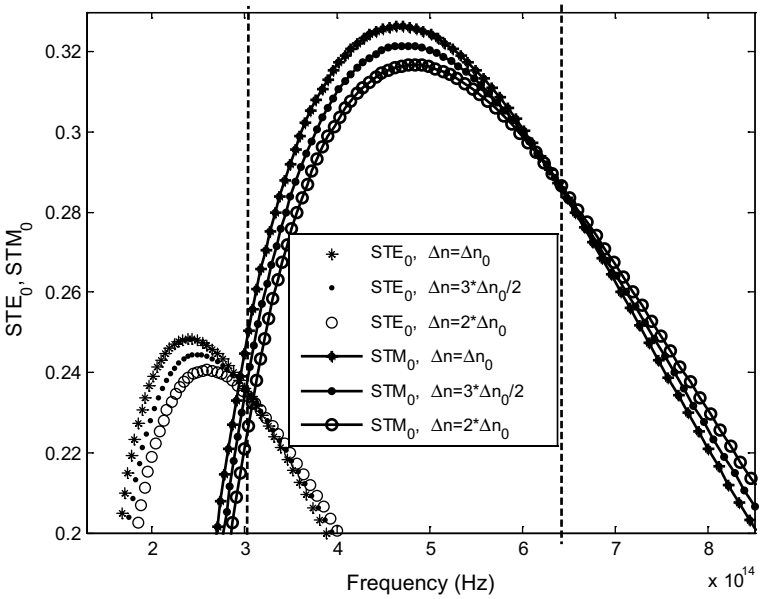

Fig. 4 TM_0 and TE_0 modes sensitivities as a function of the frequency for different value of increasing total birefringence Δn induced by different values of positive applied electric field, markers with linked lines curves for TM_0 mode and markers without linked lines curves for TE_0 mode (d = 100 nm, $n_p = 1.628$, $n_s = 1.72$, $LiNbO_3$ as guiding film)

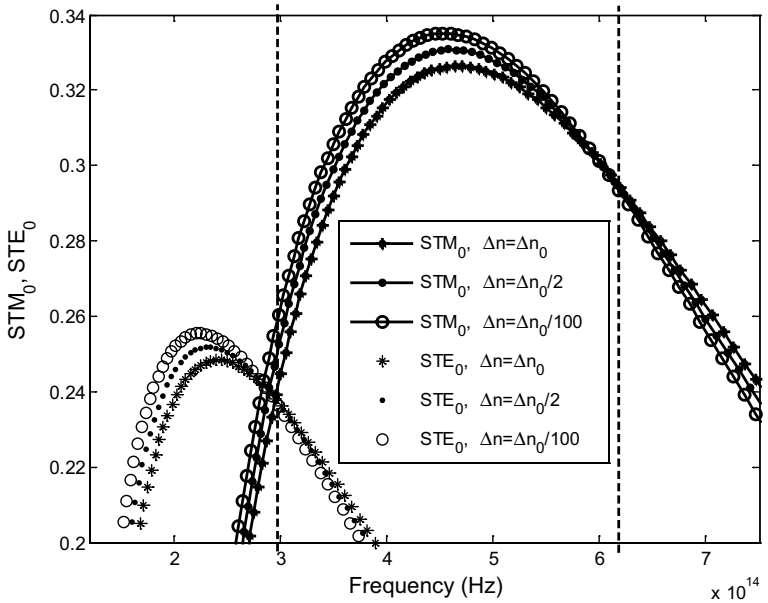

Fig. 5 Sensitivities as a function of the frequency for different value of decreasing total birefringence Δn induced by different values of negative applied electric field, markers with linked lines curves for TM_0 mode and markers without linked lines curves for TE_0 mode (d = 100 nm, $n_p = 1.628$, $n_s = 1.72$, $LiNbO_3$ as guiding film)

two different behaviors; the first behavior occurs before the frequencies 3.1e−14 Hz and 6.2e−14 Hz for TE_0 and TM_0 modes successively, whereas, the second behavior occurs beyond these two frequencies. For positive applied E-field (Fig. 4) and before the mentioned frequencies, the increase the electric field induces an increase in the total anisotropy, which causes the decrease of the sensor sensitivity particularly around the maximum. However, for negative applied E-field (Fig. 5), the increase of the absolute values of electric field induces a decrease in the total anisotropy, which causes an increase in the sensor

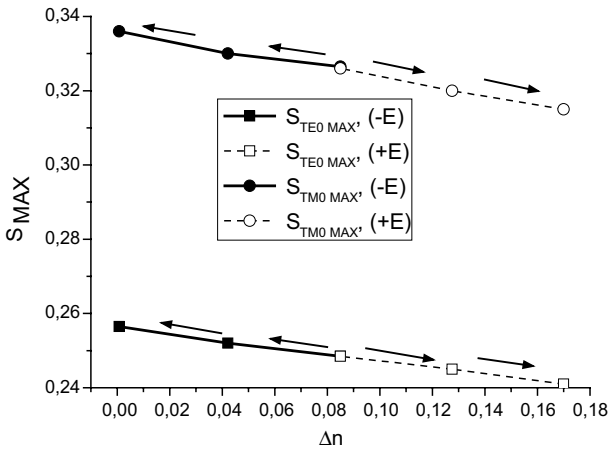

Fig. 6 Maximum sensitivity variation as a function of total birefringence Δn for: positive applied E-Field (dashed lines), negative applied E-Field (solid lines), square solid and dashed lines for TE_0 mode and circle solid and dashed lines for TM_0 mode (d = 100 nm, $n_p = 1.628$, $n_s = 1.72$, $LiNbO_3$ as guiding film)

sensitivity on the vicinity of the maximum. On the other hand, beyond the previous frequencies, the increase of the electric field induces an increase in the sensor sensitivity (positive E-field case), while, the increase of absolute values of electric field induces a decrease in the sensor sensitivity (negative E-field case). Our interest focuses on the intervals where the sensitivities are maximal, which means, the near infrared domain for TE_0 mode and the visible frequency domain for TM_0 mode.

Figure 6 presents maximum fundamental modes sensitivities changes as a function of total birefringence Δn for positive and negative applied E-Field. The figure shows the decreasing of maximum sensitivity according to the increasing of anisotropy (dashed lines), and the increasing of maximum sensitivity according to the decreasing of anisotropy (solid lines). Further, the figure shows well that the sensitivities of TM_0 mode (circle solid and dashed lines) are greater than those of TE_0 mode (square solid and dashed lines). Moreover the sensitivities in the case of negative electric field (solid lines) are more important than those in the case of positive electric field (dashed lines). The difference between the two maximum sensitivities corresponding to the two extremes values of Δn are approximately 7.5e−3 and 9.0e−3 for TE_0 and TM_0 modes respectively, for both positive and negative applied electric field. It appears that the maximum sensitivity changes as a function of anisotropy for TM_0 mode are greater than those of TE_0 mode.

4 Conclusions

In this work we have studied the sensitivity of a planar waveguide sensor based on evanescent wave interactions constituted by uniaxial birefringent materials. We have calculated the sensor sensitivity formulas for the two kinds of modes propagating simultaneously in its waveguide. Then, we have studied the influence of the physical parameters of the planar waveguide on the sensor sensitivity (the core of the waveguide is the $LiNbO_3$). The results show that there are two possibilities to increase the sensitivities (for a fixed thickness); the first possibility is to use an isotropic substrate instead of a birefringent substrate. The other possibility is to make the substrate index as close as possible to the measurand index. Noting that, physical parameters also shift sensitivity curves to or away from visible frequencies.

On the other hand, we have studied the influence of E-field induced birefringence of the wave guiding film ($LiNbO_3$), on the sensitivity of the studied sensor for TE_0 and TM_0 modes. In our study we have distinguished between two different cases. The first case when the electric field is applied along the optic axis (+c) of the $LiNbO_3$ wave guiding film (positive electric field); the second case when the electric field is applied opposite to the optic axis (−c) of such uniaxial crystal (negative electric field). The obtained results showed that, for positive electric field, the increase of electric field induces an increasing of the total anisotropy which causes a decreasing on the sensor sensitivity particularly around the maximum. However, for negative electric field, the increase of absolute values of negative electric field induces the decrease of the total anisotropy which causes an increasing on the sensor sensitivity on the vicinity of the maximum.

Funding This project is funded by: Research Unity in Optics and Photonics – University of Setif 1, Center of development of advanced technologies, Algiers, Algeria.

References

Alkanoo, A.A., Taya, S.A.: Theoretical investigation of five-layer waveguide structure including two left-handed material layers for refractometric applications. J. Magn. Magn. Mater. **449**(1), 395–400 (2018)

Densmore, A., Xu, D.X., Waldron, P., Janz, S., Cheben, P., Lapointe, J., Delâge, A., Lamontagne, B., Schmid, J.H., Post, E.: A silicon-on-insulator photonic wire based evanescent field sensor. IEEE Photonics Technol. Lett. **18**(23), 2520–2522 (2006)

Dutta, A., Deka, B., Sahu, P.P.: Planar Waveguide Optical Sensors, from Theory to Applications. Springer, Cham (2016)

Horvath, R., Pedersen, H.C., Skivesen, N., Selmeczi, D., Larsen, N.B.: Optical waveguide sensor for on-line monitoring of bacteria. Opt. Lett. **28**(14), 1233–1235 (2003)

Huang, Y., Kalyoncu, S.K., Zhao, Q., Torun, R., Boyraz, O.: Silicon-on sapphire waveguides design for mid-IR evanescent field absorption gas sensors. Opt. Commun. **313**, 186–194 (2014)

Jalaleddine, A.M.: Guided waves propagating in isotropic and uniaxial anisotropic slab waveguide. Dissertation, Ohio University, USA (1982)

Kovalevich, T., Belharet, D., Robert, L., Kim, M.S., Herzig, H.P., Grosjean, T., Bernal, M.P.: Experimental evidence of Bloch surface waves on photonic crystals with thin-film $LiNbO_3$ as a top layer. Photonics Res. **5**(6), 649–653 (2017)

Kumar, D., Singh, V.: Theoretical modeling of a nonlinear asymmetric metal-clad planar waveguide based sensors. Optik **122**(20), 1872–1875 (2011)

Levy, M., Osgood Jr., R.M., Liu, R., Cross, L.E., Cargill III, G.S., Kumar, A., Bakhru, H.: Fabrication of single-crystal lithium niobate films by crystal ion slicing. Appl. Phys. Lett. **73**(16), 2293–2295 (1998)

Mukundan, H., Anderson, A.S., Grace, W.K., Hartman, N., Martinez, J.S., Swanson, B.I.: Waveguide-based biosensors for pathogen detection. Sensors **9**(7), 5783–5809 (2009)

Parriaux, O., Dierauer, P.: Normalized expressions for the optical sensitivity of evanescent wave sensors. Opt. Lett. **19**(20), 508–510 (1994)

Rabieia, P., Gunter, P.: Optical and electro-optical properties of submicrometer lithium niobate slab waveguides prepared by crystal ion slicing and wafer bonding. Appl. Phys. Lett. **85**(20), 4603–4605 (2004)

Ranacher, C., Consani, C., Maier, F.J., Hedenig, U., Jannesari, R., Lavchiev, V., Tortschanoff, A., Grille, T., Jakoby, B.: Spectroscopic gas sensing using a silicon slab waveguide. Procedia Eng. **168**, 1265–1269 (2016)

Saleh, E.A., Teich, M.C.: Electro-optics. In: Saleh, E.A., Teich, M.C. (eds.) Fundamentals of Photonics, pp. 696–736. Wiley, Hoboken (1991)

Taya, S.A.: Slab waveguide with air core layer and anisotropic left-handed material claddings as a sensor. Opto-Electron. Rev. **22**(4), 252–257 (2014)

Taya, S.A.: P-polarized surface waves in a slab waveguide with left-handed material for sensing applications. J. Magn. Magn. Mater. **377**, 281–285 (2015a)

Taya, S.A.: Theoretical investigation of slab waveguide sensor using anisotropic metamaterials. Opt. Appl. **45**(3), 405–417 (2015b)

Taya, S.A.: Ternary photonic crystal with left-handed material layer for refractometric application. Opto-Electron. Rev. **26**(3), 236–241 (2018)

Taya, S.A., Shaheen, S.A.: Binary photonic crystal for refractometric applications (TE case). Indian J. Phys. **92**(4), 519–527 (2018)

Taya, S.A., Shabat, M.M., Khalil, H.M.: Enhancement of sensitivity in optical waveguide sensors using left-handed materials. Optik **120**(10), 504–508 (2009)

Timtere, P., Usman, A., Ododo, J.C.: The phenomenon of nonlinear optical birefringence in uniaxial crystals. Lat. Am. J. Phys. Educ. **5**(2), 432–437 (2011)

Veldhuis, G.J., Parriaux, O., Hoekstra, H.J.W.M., Lambeck, P.V.: Sensitivity enhancement in evanescent optical waveguide sensors. J. Lightwave Technol. **18**(5), 677–682 (2000)